Macromolecules
ARTICLE

Macromolecules **2009**, *42*, 5339–5344 **5339**
DOI: 10.1021/ma900740b

Association of Block Copolymer in Nonselective Solvent

Fuyou Ke,[†] Xiulei Mo,[†] Runmiao Yang,[‡] Yanmei Wang,*[,‡] and Dehai Liang*[,†]

[†]*Beijing National Laboratory for Molecular Sciences, Department of Polymer Science and Engineering and the Key Laboratory of Polymer Chemistry and Physics of the Ministry of Education, College of Chemistry and Molecular Engineering, Peking University, Beijing 100871, China, and* [‡]*Department of Polymer Science and Engineering, University of Science and Technology of China, Hefei 230026, China*

Received April 6, 2009; Revised Manuscript Received May 15, 2009

ABSTRACT: The behavior of poly(ethylene oxide)-*block*-poly(*N*,*N*-dimethylacrylamide) (PEO-*b*-PDMA) in aqueous solution at dilute concentrations was studied by laser light scattering. Even though water was a nonselective solvent for both PEO and PDMA blocks, PEO-*b*-PDMA formed a certain loose associate in aqueous solutions. Different from the micellization of block copolymers in selective solvents, the association of PEO-*b*-PDMA in aqueous solution showed weak concentration and temperature dependence as well as opposite salt effect. At 4.0 M NaCl, the association was completely suppressed and PEO-*b*-PDMA existed as individual polymer chains. This opposite "salting out" effect revealed the association mechanism of block copolymers in nonselective solvent: the solubility of PEO block in aqueous solution was unique, and it exhibited a better hydrophilicity and thick hydration shell than other water-soluble polymers. This inequality or weak incompatibility drove the block copolymer to associate into loose structures containing multidomains rich of either blocks. The dependence of the association on the block ratio also supported our conclusions.

Introduction

Block copolymers have been widely studied in the past 20 years, mainly because of their capacity of forming diverse morphologies in the solvents selective for one of the blocks. A variety of ordered structures, including spheres, vesicles, cylinders, and lamellae, have been assembled by the control of the synthetic chemistry, the external conditions (e.g., concentration and temperature), and the kinetics.[1−6] These well-defined structures render block copolymers many practical applications in the fields of thermoplastic elastomers, solubilizers, dispersion agents, nanomaterials, and so on.[3,7−13] More recently, the block copolymers containing poly(ethylene oxide) (PEO) are drawn much attention in drug (gene) delivery due to their good biocompatibility and some other superior properties.[14−20]

When block copolymer is dissolved in a nonselective solvent, i.e, a solvent good for all the blocks, the copolymer is generally considered to exist as single chains. Because of the unfavorable thermodynamic interactions between different blocks, the single polymer chains may adopt segregated conformation, core−shell conformation, or some conformation in between.[21−24] Recently, Topp et al. observed that PEO-*b*-poly(*N*-isopropylacrylamide) (PNIPAM) formed aggregates in aqueous solution at temperatures below the low critical solution temperature (LCST) of PNIPAM.[25] Annaka and co-workers also reported that the "disordered micelles" formed by PEO-*b*-PNIPAM was started at temperature as low as 17 °C, far below the critical micelle temperature.[26] With increasing temperature to induce the collapse of PNIPAM chains, the "abnormal" aggregate disassociated with a certain extent before the formation of micelles.[27]

Edelmann et al. investigated the aggregation behavior of PEO-*b*-poly(methyl methacrylate) (PEO-*b*-PMMA) in nonselective solvents, such as tetrahydrofuran (THF), acetone, chloroform, 1,4-dioxane, and 2,2,2-trifluoroethanol.[28] The good solvent quality was assured by the positive A_2 values and the calculated Flory−Huggins interaction parameters, χ, whose values were less than 0.5 for all the solvents. An aggregate with the size at least one order larger than that of the single chain was detected by the scattering techniques in all the solutions except in 1,4-dioxane. The measurements on the surface tension and ^{1}H NMR also demonstrated that the aggregate was not micellar structures. The authors attributed the aggregation to certain strongly fluctuating and internally disordered objects.[28]

Clearly, the block copolymers, at least PEO-containing block copolymers, were not in the state of single polymer chains in nonselective solvent. They formed a certain kind of aggregate or associate with an unclear reason. In the present work, we synthesized the diblock copolymers of PEO-*b*-poly(*N*,*N*-dimethylacrylamide) (PEO-*b*-PDMA) with different block ratio by using the atom transfer radical polymerization (ATRP) and studied the aggregation behavior of PEO-*b*-PDMA in detail in aqueous solution by the combination of dynamic and static light scattering. To reveal the mechanism of aggregation, we focused on the effect of block ratio, concentration, temperature, salt concentration, and the aggregation behavior in organic solvent and in the presence of homo-PEO chains.

Experimental Section

Materials. THF and NaCl were purchased from Beijing Chemical Reagent Co. (Beijing, China) and used as received. Milli-Q water (Millipore) with resistance of 18.2 MΩ was used throughout the experiments.

Synthesis of PEO-*b*-PDMA. Five PEO-*b*-PDMA samples with different block ratio were synthesized by ATRP with CuBr and 5,5,7,12,12,14-hexamethyl-1,4,8,11-tetraazamacrocyclotetradecane (Me_6[14]aneN_4) as the catalyst and ligand, respectively.[29] PEO-Br macroinitiator was synthesized by esterification of PEO (molecular mass 2000) with 2-bromoisobutyryl bromide. The ratio of PEO-Br/CuBr/Me_6[14]aneN_4 was kept

*Corresponding authors: Tel 86-551-3607652, e-mail wangyanm@ustc.edu.cn (Y.W.); Fax +86-10-62756170, e-mail dliang@pku.edu.cn (D.L.).

Published on Web 06/05/2009

Table 1. Molecular Weight and Polydispersity of PEO-*b*-PDMA

molecular formula	M_n(NMR)	M_w/M_n(GPC)
PEO_{44}-*b*-$PDMA_{49}$	7000	1.2
PEO_{44}-*b*-$PDMA_{88}$	11000	1.2
PEO_{44}-*b*-$PDMA_{173}$	19000	1.2
PEO_{44}-*b*-$PDMA_{216}$	23000	1.2
PEO_{44}-*b*-$PDMA_{304}$	32000	1.3

constant at 1/1/3. The reagents were added in a dried glass tube together with monomer (DMA) and toluene. After degassing by three freeze−pump−thaw cycles, the tube was sealed under vacuum and then immersed in a water bath thermostated at 20 °C. The reaction was carried out for a prescribed time period. The polymer samples were then taken out and dissolved in DMF. An alumina column was used to remove copper. The polymer product in DMF was precipitated by adding excess amount of ether and then filtered and dried at 40 °C in a vacuum oven for 24 h. The molecular weight of the resulting PDMA was controlled by the initial feed ratio of DMA to PEO-Br and the conversion of DMA. The molecular weight of the resulting PDMA increased linearly with the conversion of the DMA.[29]

The molecular weight distribution of PEO-*b*-PDMA were measured by using a gel permeation chromatography (GPC) system, which was equipped with a Waters 2410 refractive index detector, a Waters 515 HPLC pump, and three Waters Styragel Columns (HT2, HT3, and HT4). The columns were thermostated at 35 °C. Linear polystyrene standards were used for calibration. THF at a flow rate of 1.0 mL/min was used as the eluent. ^{1}H NMR was conducted in an AV-300 NMR spectrometer at 20 °C by using D_2O as the solvent. The average molecular weight and the block ratio were determined by using the peak integral of the $-OCHH_2CH_2-$ protons of PEO and the *N*-methyl protons of DMA units. The results from GPC and ^{1}H NMR are summarized in Table 1.

Sample Preparation. The stock solution of each block copolymer was prepared by directly dissolving the polymer powder in the solvents and allowing it to stay overnight to ensure complete dissolution. The resulting stock solution was then diluted into desired concentration with proper amount of solvents. For LLS measurements, the solution was filtered through a 0.45 μm Millipore filter into a dust-free vial.

LLS. A commercialized LLS spectrometer from Brookhaven Instruments Corp. (Holtsville, NY) was used to perform both static light scattering (SLS) and dynamic light scattering (DLS) over a scattering angular range of 20°−120°. A solid-state laser (532 nm, 100 mW, CNI Changchun GXC-III, China) polarized at the vertical direction was used as the light source, and a BI-TurboCorr digital correlator was used to collect and process data. In SLS, the angular dependence of the excess absolute time-averaged scattered intensity, also known as the Rayleigh ratio $R_{vv}(\theta)$, was measured. For a very dilute solution, the weight-averaged molar mass (M_w) and the root mean-square radius of gyration (R_g) can be obtained on the basis of

$$HC/R_{vv}(\theta) = (1/M_w)[1 + (1/3)R_g{}^2q^2] + 2A_2C \quad (1)$$

where $H = 4\pi^2n^2(dn/dC)^2/(N_A\lambda^4)$ and $q = 4\pi n/\lambda \sin(\theta/2)$ with N_A, C, n, dn/dC, and λ being Avogadro's number, the concentration, the solvent refractive index, the specific refractive index increment, and the wavelength of light in a vacuum, respectively. In dynamic LLS, the intensity−intensity time correlation function $G^{(2)}(\tau)$ in the self-beating mode was measured

$$G^{(2)}(\tau) = A[1 + \beta|g^{(1)}(\tau)|^2] \quad (2)$$

where A is the measured baseline, β is a coherence factor, τ is the delay time, and $g^{(1)}(\tau)$ is the normalized first-order electric field time correlation function. $g^{(1)}(\tau)$ is related to the line width distribution $G(\Gamma)$ by

$$g^{(1)}(\tau) = \int_0^\infty G(\Gamma)e^{-\Gamma\tau}\,d\Gamma \quad (3)$$

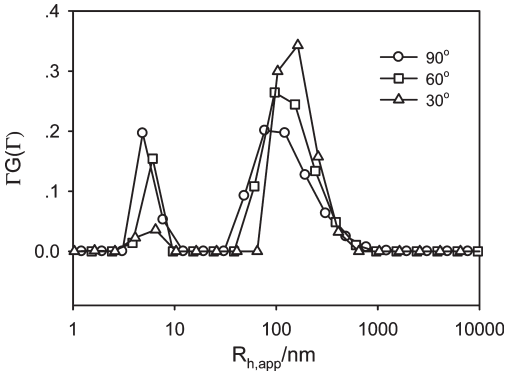

Figure 1. Size distribution of PEO_{44}-*b*-$PDMA_{173}$ in water at 1.3 mg/mL.

By using a Laplace inversion program, CONTIN, the normalized distribution function of the characteristic line width $G(\Gamma)$ was obtained. The average line width, $\bar{\Gamma}$, was calculated according to $\bar{\Gamma} = \int\Gamma G(\Gamma)\,d\Gamma$. $\bar{\Gamma}$ is a function of both C and q, which can be expressed as

$$\bar{\Gamma}/q^2 = D(1 + k_dC)[1 + f(R_gq)^2] \quad (4)$$

with D, k_d, and f being the translational diffusive coefficient, the diffusion second virial coefficient, and a dimensionless constant, respectively. D can be further converted into the hydrodynamic radius R_h by using the Stokes−Einstein equation:

$$D = k_BT/6\pi\eta R_h \quad (5)$$

where k_B, T, and η are the Boltzmann constant, the absolute temperature, and the viscosity of the solvent, respectively.

Determination of d*n*/d*C*. The dn/dC of the block copolymers was calculated by $dn/dC = w_1(dn/dC)_1 + w_2(dn/dC)_2$, with w_1 and w_2 denoting the weight fraction of PEO and PDMA blocks, respectively. The dn/dC values of the homopolymers in the corresponding solvents were obtained either from ref 31 or from the measurement by a differential refractometer (Wyatt Optilab Rex). It was determined that the dn/dC values of PEO and PDMA in 1 M NaCl were ca. 0.12 and 0.14 mL/g, respectively. The dn/dC value of PDMA in THF was determined to be 0.068 mL/g, close to the value of PEO in the same solvent.[31] The refractive index of 1 M NaCl is 1.34.

Results and Discussion

Associates in Aqueous Solution. Water is known as a good solvent for both PEO and PDMA at room temperature. Individual PEO or PDMA chains in the swollen state are expected in dilute aqueous solutions. Figure 1 shows the size distribution of PEO_{44}-*b*-$PDMA_{173}$ in water at 1.3 mg/mL. Two characteristic diffusive modes, with the peak $R_{h,app}$ values at 5.4 and 147 nm, respectively, were observed. Considering that there were only 217 repeating units in PEO-*b*-PDMA, we attributed the fast diffusive mode to the single molecules of copolymer and the slow mode to the aggregates formed by PEO_{44}-*b*-$PDMA_{173}$ in aqueous solution. Since the aggregate was in equilibrium with the single polymer chains, it was more proper to call it "associates", as suggested by Elias.[30] According to eqs 2 and 3, the size distributions in Figure 1 were averaged by intensity. Because the scattered intensity was roughly proportional to the sixth power of the size, the number of the large associates in the

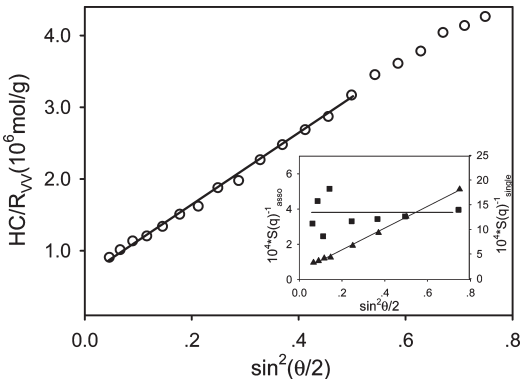

Figure 2. SLS result of PEO_{44}-*b*-$PDMA_{173}$ in water at 1.3 mg/mL. The inset shows the static structure factors of the single chains (solid square) and the associate (solid triangle).

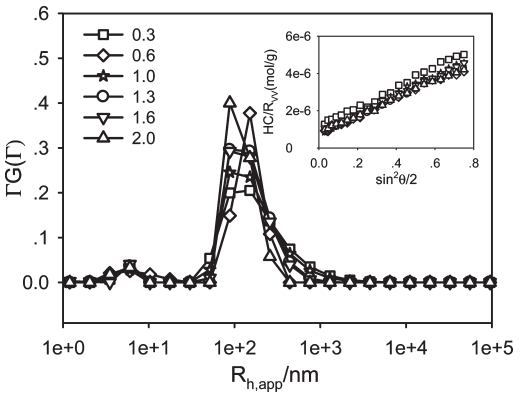

Figure 3. Size distribution of PEO_{44}-*b*-$PDMA_{173}$ at different concentrations at 30°. The inset shows concentration dependence of the excess scattered intensity.

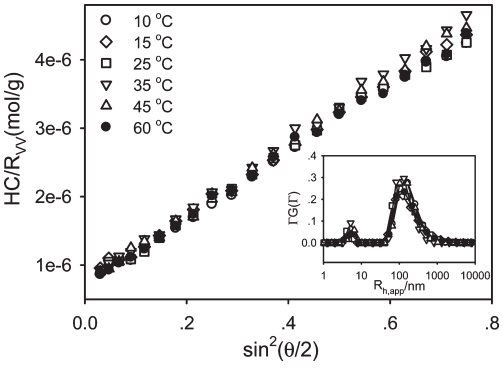

Figure 4. Angular dependence of the excess scattered intensity of PEO_{44}-*b*-$PDMA_{173}$ at 1.3 mg/mL at varying temperatures. The inset shows the size distribution at 30°.

system was much less than that of the individual chains. The formation of the associates was also demonstrated by SLS. The dn/dC values of PEO and PDMA in aqueous solution were large and close (0.135−0.15 mL/g).[31] Therefore, the apparent molecular weigh could be evaluated from the angular dependence of the excess scatted intensity. By using the data point below 90°, a $M_{w,app}$ of 1.6×10^6 g/mol, ~80 times larger than the single polymer chains, was obtained after the extrapolation to zero angle. The fitting of the curve (the fitting coefficient $r^2 > 0.99$) in Figure 2 also yielded a $R_{g,app}$ of ~153 nm, much larger than the size of single PEO_{44}-*b*-$PDMA_{173}$ chain. (The values of $M_{w,app}$ and $R_{g,app}$ obtained in this approach are used only to indicate the degree of association; they do not have much physical meanings.) Both DLS and SLS results proved the association of PEO-*b*-PDMA in aqueous solution.

According to Sato and co-workers,[32] the static structure factors ($S(q)$) of the fast mode and the slow mode were able to be calculated separately, by the combination of the SLS and DLS data. The radius of gyration was then obtained from the $S(q)$. By using the scattering data at 30°, 35°, 40°, 45°, 60°, 75°, 90°, and 120°, we calculated the $S(q)$ of the slow mode and the fast mode, which is shown in the inset in Figure 2. The structure factor of the fast mode shows a horizontal line, indicating that the scattered intensity from the single polymer chain has no angular dependence. The large fluctuation at low angle was due to the smaller area ratio of the fast mode (Figure 1). However, the $S(q)$ of the associate exhibits a strong angular dependence, and the $R_{g,app}$ of 204 nm was obtained. The conformation of the associate was inferred from the R_g/R_h ratio. It was well established in literature that the R_g/R_h ratios were 0.775 and 1.5 for solid sphere and random coil, respectively.[33] The $R_{g,app}/R_{h,app}$ ratio of the associate formed by PEO_{44}-*b*-$PDMA_{173}$ in aqueous solution was ~1.4, much larger than 0.775, indicating that the associate was in a loose conformation, close to random coil. It was definitely not micellar structures, which agreed with the findings by Edelmann et al.[28] Given that the bond lengths of C−C and C−O were 0.154 and 0.143 nm, respectively, the contour length of PEO_{44}-*b*-$PDMA_{173}$ was calculated to be ~50 nm, much smaller than the radius of the associate, suggesting that the associate was composed of multidomains rich of either PEO or PDMA chains.

Concentration Effect. Figure 3 shows the size distribution of PEO_{44}-*b*-$PDMA_{173}$ at different concentrations. At concentrations below 0.1 mg/mL, the association was hardly detected by LLS. With increasing concentration to 0.6 mg/mL, the associate became stronger, as demonstrated by the results from DLS and SLS (Figure 3). And no apparent changes on the association were observed thereafter. As shown in the inset in Figure 3, the $M_{w,app}$ fluctuated from 1.2×10^6 to 1.5×10^6 g/mol and the $R_{g,app}$ kept almost constant at ~140 nm in the concentration range of 0.6−2.0 mg/mL. Hence, it was concluded that the associate had a weak concentration dependence once it was developed.

Temperature Effect. It was generally believed that concentration and temperature were two major effects on the micellization of block copolymers in selective solvents. At certain temperature, there existed the concentration, known as cmc, above which the block copolymers formed micelles. On the other hand, at a given concentration, there existed a temperature, known as cmt, above or below which the micellization occurred. As discussed above, the concentration dependence of PEO_{44}-*b*-$PDMA_{173}$ in aqueous solution was different (Figure 3) from the behavior of the block copolymer in a selective solvent. Besides the concentration, the temperature also affected the association of PEO_{44}-*b*-$PDMA_{173}$ in a way quite different from its effect on the micellization. As show in Figure 4, no apparent changes in $M_{w,app}$ and $R_{g,app}$ was observed for PEO_{44}-*b*-$PDMA_{173}$ in aqueous solution at temperatures ranging from 10 to 60 °C. The inset in Figure 4 also shows that the size and size distribution of the single polymer chains, and the associates are almost constant as the rise of the temperature from 10 to 60 °C, indicating the weak dependence of the associate on the temperature.

Effect of Block Ratio. Keeping the molecular weight of PEO (2K) constant, we also studied the association behavior of PEO-*b*-PDMA with different PDMA length. Figure 5 shows the DLS results of PEO-*b*-PDMA in aqueous solution at 1.3 mg/mL at 30°. The sizes of the fast mode, which shows

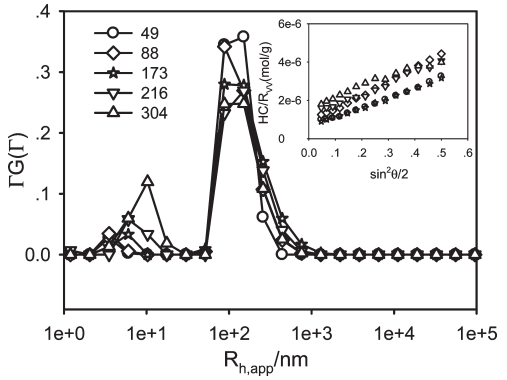

Figure 5. Effect of block ratio on the association of PEO_{44}-*b*-PDMA at 1.3 mg/mL at 30°. The inset shows the SLS data.

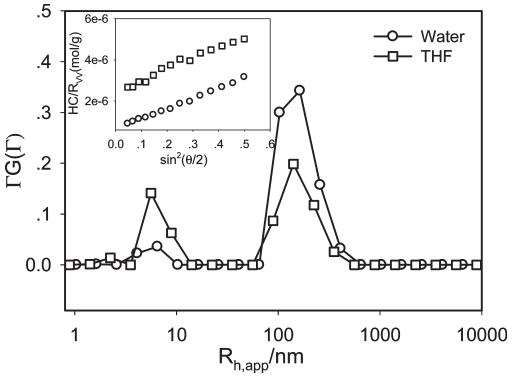

Figure 6. Association of PEO_{44}-*b*-$PDMA_{173}$ in THF at 1.3 mg/mL at 30°.

no angular dependence, increases with the length of PDMA block. The $R_{h,app}$ values are summarized in Table 2. Figure 5 also indicated that the association becomes weak as the length of PDMA block increases. This phenomenon also conflicted with the behavior of block copolymer in selective solvent, where the aggregation became stronger with the increase of the core-forming block.[34] The SLS data (the inset in Figure 5) also indicated that PEO_{44}-*b*-$PDMA_{49}$ had the largest $M_{w,app}$ (1.8×10^6 g/mol) and $R_{g,app}$ (170 nm), while PEO_{44}-*b*-$PDMA_{304}$ had the smallest $M_{w,app}$ (0.54×10^6 g/mol) and $R_{g,app}$ (83 nm) under that same conditions. The values for other polymers are also listed in Table 2. The data in Figure 5 demonstrated that the association was highly dependent on the block ratio, with the short PDMA block yielding the strongest associates.

Association in Organic Solvent. To reveal the driving force for the association, we also studied the behavior of PEO_{44}-*b*-$PDMA_{173}$ in organic solvent. As shown in Figure 6, the association is much weaker in THF than that in aqueous solution. The $R_{g,app}$ and $M_{w,app}$ of PEO_{44}-*b*-$PDMA_{173}$ in THF were calculated from the SLS data in the inset in Figure 6. The $R_{g,app}$ value in THF was ~77 nm, and the $M_{w,app}$ was $\sim 0.41 \times 10^6$ g/mol. Both of the values were much smaller than those in pure water (153 nm and 1.6×10^6 g/mol, respectively). It was known that water molecule is an excellent hydrogen-bonding agent; it can strongly interact with PEO and PDMA via hydrogen bond. Good structural fit is another reason in the case of PEO.[35] But THF does not have these capacities due to the lack of hydrogen. The formation of associate in THF indicated that hydrogen bond enhanced the association.

Association Mechanism. Compared with the micellization in selective solvent, the association behavior of the block copolymer in nonselective solvent followed quite different rules in terms of concentration dependence, temperature

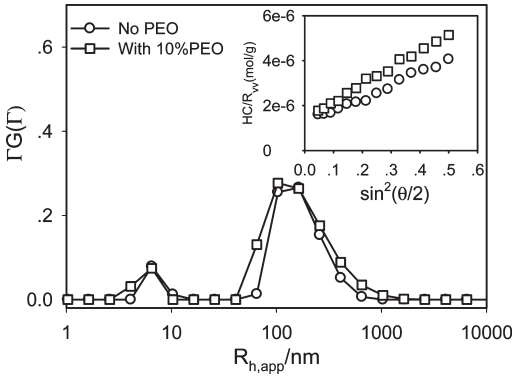

Figure 7. Effect of PEO on the association of PEO_{44}-*b*-$PDMA_{216}$ at 1.3 mg/mL at 30°. The inset compares the SLS data.

effect, and the dependence of block ratio. The association could be caused by the hydrophobic end group introduced during the synthesis. This end-group effect was prominent when the overall molecular weight of the polymer was relatively low. The end-group-induced aggregation has been observed in a number of homopolymer systems, such as PEO,[36,37] PNIPAm,[38] and poly(hydroxyethyl acrylamide).[39] For example, alkyl-terminated PNIPAms formed a hydrophobic core of alkyl chain ends as long as the alkyl end group was large enough.[40−44] Generally, the aggregation induced by end group followed the rules similar to that of micellization. In our case, PEO-*b*-PMDA was synthesized by ATRP method, and the end group was merely −Br at the PDMA end. The bromide group should generate a negligible effect on the association of the block copolymer because of its relatively small size and weak hydrophobicity.

It has been reported that the homopolymer residues during the synthesis of block copolymer caused an anomalous micellization,[45] where an aggregate with large size appeared prior to or together with the regular micelles. To test whether the association of PEO-*b*-PDMA in aqueous solution was induced by the unreacted PEO initiator, we mixed 10% (weight ratio) PEO with molecular weight of 2000 into PEO_{44}-*b*-$PDMA_{216}$ at 1.3 mg/mL. The weight ratio of PEO was almost equal to the weight ratio of the PEO initiators to the total amount of DMA monomers during the polymerization. As indicated by the GPC results (Supporting Information, Figure S1), no unreacted PEO initiators was detected in the PEO-*b*-PDMA samples. Therefore, 10 wt % was far beyond the real amount of the unreacted PEO initiators. As shown in Figure 7, the addition of PEO exhibited a weak effect on the association of PEO_{44}-*b*-$PDMA_{216}$. The $M_{w,app}$ and $R_{g,app}$ were slightly changed from 0.83×10^6 g/mol and 120 nm, respectively, to 0.77×10^6 g/mol and 127 nm after adding 10% PEO (the inset in Figure 7). Therefore, the unreacted PEO chains, if there were any, were not the driving force of the association.

On the basis of the above discussion, the origin of the association was neither the hydrophobic end groups nor the PEO initiators remained in the system. It was noticed that solvent quality, e.g., the use of THF, was able to weaken the association (Figure 6). Besides changing solvent type, the addition of salt to aqueous solution was a common method to alter the solvent quality. The salt effect has been widely investigated in the study of the Pluronics copolymers (PEO−PPO−PEO, with PPO denoting poly(propylene oxide)). Generally, the effect of anion is larger than that of the cation, and the anions can be classified into the Hofmeister series according to their "salting-out" strength at the same concentration. NaCl was considered as a strong "salting-out"

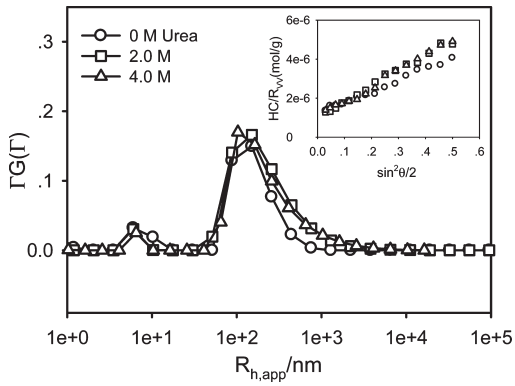

Figure 8. Effect of urea on the association of PEO_{44}-*b*-$PDMA_{173}$ at 1.3 mg/mL at 30°. The inset compares the SLS result.

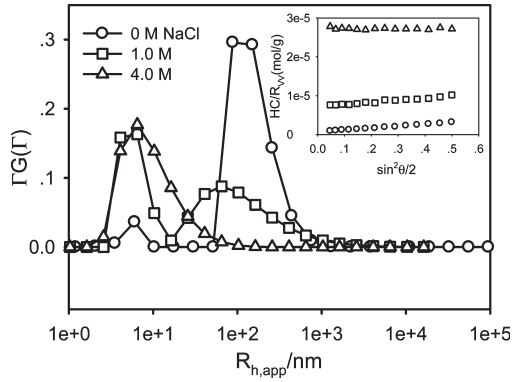

Figure 9. Effect of NaCl on the association of PEO_{44}-*b*-$PDMA_{173}$ at 1.3 mg/mL at 30°. The inset compares the SLS data.

agent. It was able to effectively decrease the cmt and the clouding point of PEO−PPO−PEO.[46] The effect of urea was opposite. It was used as a weak "salting-in" agent.

Figure 8 shows the effect of urea on the association of PEO-*b*-PDMA in aqueous solution. As urea concentration increased, the association was slightly enhanced. The SLS data (inset in Figure 8) also indicated that $M_{w,app}$ in 4.0 M urea was 0.99×10^6 g/mol and $R_{g,app}$ was 155 nm, both of which were larger than those ($M_{w,app} = 0.83 \times 10^6$ g/mol, $R_{g,app} = 120$ nm) in the solvent without urea. Therefore, urea, the "salting-in" agent in micellization, exhibited a "salting-out" effect on the association of PEO-*b*-PDMA in nonselective solvent.

The opposite trend was observed on NaCl. As shown in Figure 9, the association was greatly weakened by adding NaCl, the commonly believed "salting-out" agent. At 4.0 M NaCl, the associate was suppressed completely, and PEO_{44}-*b*-$PDMA_{173}$ stayed as individual polymer chains. Assuming that the salt concentration exhibited negligible effect on dn/dC, the SLS data in the inset in Figure 9 yielded the $M_{w,app}$ of single chain to be 3.6×10^4 g/mol. With the known $M_{w,app}$ of single chain, we can calculate the weight ratio and the $M_{w,app}$ of the associate using the data in Figure 2. The calculated results indicated that about 6% (weight ratio) of PEO_{44}-*b*-$PDMA_{173}$ chains formed the associate at 1.3 mg/mL. The $M_{w,app}$ of the associate was ca. 3.2×10^7 g/mol, corresponding to an association number of ~800.

The suppression of the associate by NaCl gained insight in the association mechanism of PEO-containing block copolymer in aqueous solutions. PEO is a polymer with some special properties. It is soluble in both organic solvent and water. The solubility of PEO in water is kind of unique, where the polymer exhibited a good fit to the water structure.[35] Such coupling led to a decrease in thermal motion and hence a mutual stabilization. The mechanism of "salting-in" or "salting-out" effect is not explicit from the literature. According to the explanation by Florin et al.,[47] the ions from the salt polarized the water molecules surrounding them, resulting in a low free energy. Since PEO has a less tendency to attract ions than water, the structural fit of water and PEO now became unfavorable due to the entropic contribution. The removal of water from the PEO hydration shell resulted in an attractive PEO−PEO interaction.[46] The effect of salt on the solubility of PEO in aqueous solution has been studied by either laser light scattering[48] or membrane osmometry.[49] The obtained second viral coefficient A_2 drastically reduced with increasing concentration of NaCl or KCl, suggesting that the interaction between PEO and water was weakened. In the case of micellization by Pluronics copolymers containing a hydrophobic block, the weakening of the hydrophilicity of PEO chain decreased the transition point and cmt. In our case, the other block is hydrophilic; the addition of NaCl should even the hydrophilicity of PEO and PDMA and thus prevent the formation of associates.

Table 2. LLS Results of PEO-*b*-$PDMA_n$ at 1.3 mg/mL

number of DMA	49	88	173	216	304
$R_{h,app}$/nm (single chain)	3.8	4.1	5.4	6.2	8.2
$R_{h,app}$/nm (associate)	129	139	147	156	143
$R_{g,app}$/nm	170	166	152	114	83
$10^6 M_{w,app}$/(g/mol)	1.78	1.24	1.54	0.80	0.54

In brief, the solubility of PEO in water was different from the solubility of other hydrophilic polymers. The coupling of PEO into the water structure rendered PEO a better hydrophilicity or a thick hydration shell than other water-soluble polymers. Such incompatibility drove the PEO-containing block copolymer to associate in water. Since PEO was the main driving force, the association was closely related with the PEO/PDMA block ratio. As shown in Figure 5 and Table 2, a higher PEO ratio led to stronger association. On the other hand, the good structure fit of PEO and water, and consequently the association of the block copolymer, was less dependent on concentration and temperature to a certain extent.

If the block other than PEO had an improved ability to attract water, the association should break down. Recently, He et al. studied the association behavior of four arm PEO-*b*-poly(methacrylic acid) (PMAA) block copolymer in aqueous solution at various pH. When PMAA block was highly charged at high pH, only single polymer chains was observed from DLS at 0.1 M NaCl.[50] So far, the reported block copolymers, which formed strong associates in nonselective solvents, all contained PEO block.[25−28,51] In principle, if the blocks in a copolymer or the segments in a homopolymer exhibited different capacity interacting with the solvent molecules, the induced incompatibility would result in the association with varying degree. This is probably the reason for the association of PEO_{44}-*b*-$PDMA_{173}$ in THF, which is a good solvent for both blocks (Figure 6).

Conclusions

Block copolymers of PEO-*b*-PDMA in nonselective solvent did not exist as single polymer chains at dilute solution. They formed a certain loose associate consisting of multidomains rich of one block or another. The major driving force for the association was the incompatibility between the two blocks, mainly caused by their different capacity of interacting with solvent molecules. Compared with the micellization in selective solvent, the association of the block copolymer in nonselective solvent at dilute concentrations exhibited some distinct features: weak concentration and temperature dependence, opposite salt

effect, and so on. The study on the association of block copolymers helped in determining the molecular weight of block copolymers by light scattering and viscometry. It also shed light on the phase behavior of mixtures containing both homopolymers and block copolymers at different concentrations.

Acknowledgment. Financial support of this work from the National Natural Science Foundation of China (#20504001) is gratefully acknowledged.

Supporting Information Available: GPC curve. This material is available free of charge via the Internet at http://pubs.acs.org.

References and Notes

(1) Zhang, L.; Eisenberg, A. *Science* **1995**, *268*, 1728–1731.
(2) Discher, D. E.; Eisenberg, A. *Science* **2002**, *297*, 967–973.
(3) Riess, G. *Prog. Polym. Sci.* **2003**, *28*, 1107–1170.
(4) Jean-Francois, G. *Adv. Polym. Sci.* **2005**, *190*, 65–136.
(5) Cui, H.; Chen, Z.; Zhong, S.; Wooley, K. L.; Pochan, D. J. *Science* **2007**, *317*, 647–650.
(6) Darling, S. B. *Prog. Polym. Sci.* **2007**, *32*, 1152–1204.
(7) Morkved, T. L.; Lu, M.; Urbas, A. M.; Ehrichs, E. E.; Jaeger, H. M.; Mansky, P.; Russell, T. P. *Science* **1996**, *273*, 931–933.
(8) Fasolka, M. J.; Mayes, A. M. *Annu. Rev. Mater. Res.* **2001**, *31*, 323–355.
(9) Yu, C.; Tian, B.; Liu, X.; Fan, J.; Yang, H.; Zhao, D. Y. *Ser. Chem. Eng.* **2004**, *4*, 14–46.
(10) Ruzette, A.-V.; Leibler, L. *Nat. Mater.* **2005**, *4*, 19–31.
(11) Meier-Haack, J.; Taeger, A.; Vogel, C.; Schlenstedt, K.; Lenk, W.; Lehmann, D. *Sep. Purif. Technol.* **2005**, *41*, 207–220.
(12) Segalman, R. A. *Mater. Sci. Eng., R* **2005**, *R48*, 191–226.
(13) Bockstaller, M. R.; Mickiewicz, R. A.; Thomas, E. L. *Adv. Mater.* **2005**, *17*, 1331–1349.
(14) Allen, C.; Maysinger, D.; Eisenberg, A. *Colloids Surf., B* **1999**, *16*, 3–27.
(15) Kakizawa, Y.; Kataoka, K. *Adv. Drug Delivery Rev.* **2002**, *54*, 203–222.
(16) Torchilin, V. P. *Expert Opin. Ther. Pat.* **2005**, *15*, 63–75.
(17) Adams, M. L.; Lavasanifar, A.; Kwon, G. S. *J. Pharm. Sci.* **2005**, *94*, 1160.
(18) Gaucher, G.; Dufresne, M.-H.; Sant, V. P.; Kang, N.; Maysinger, D.; Leroux, J.-C. *J. Controlled Release* **2005**, *109*, 169–188.
(19) Alexander, K.; Jian, Z.; Valery, A. *Adv. Genet.* **2005**, *53*, 231–261.
(20) Kwon, G. S.; Forrest, M. L. *Drug Dev. Res.* **2006**, *67*, 15–22.
(21) Hadjichristidis, N.; Pispas, S.; Floudas, G. *Block Copolymers*; John Wiley & Sons: New York, 2003.
(22) Ho-Duc, N.; Prud'homme, J. *J. Int. J. Polym. Mater.* **1976**, *4*, 303.
(23) Hadjichristidis, N.; Roovers, J. *J. Polym. Phys. Ed.* **1978**, *16*, 851.
(24) Han, C.; Mozer, B. *Macromolecules* **1977**, *10*, 44–51.
(25) Topp, M. D. C.; Dijkstra, P. J.; Talsma, H.; Feijen, J. *Macromolecules* **1997**, *30*, 8518–8520.
(26) Motokawa, R.; Morishita, K.; Koizumi, S.; Nakahira, T.; Annaka, M. *Macromolecules* **2005**, *38*, 5748–5760.
(27) Yan, J.; Ji, W.; Chen, E.; Li, Z.; Liang, D. *Macromolecules* **2008**, *41*, 4908–4913.
(28) Edelmann, K.; Janich, M.; Hoinkis, E.; Pyckhout-Hintzen, W.; Horing, S. *Macromol. Chem. Phys.* **2001**, *202*, 1638–1644.
(29) Yang, R.; Shi, R.; Zhou, D.; Wang, Y.; Han, Y. *e-Polym.* **2007**, *72*.
(30) Huglin, M. B. *Light Scattering from Polymer Solution*; Academic Press: London, 1972.
(31) Brandrup, J.; Immergut, E. H.; Grulke, E. A. *Polymer Handbook*, 4th ed.; John Wiley & Sons: New York, 1999.
(32) Kanao, M.; Matsuda, Y.; Sato, T. *Macromolecules* **2003**, *36*, 2093–2102.
(33) Burchard, W. *Adv. Polym. Sci.* **1983**, *48*, 1–123.
(34) Astafieva, I.; Zhong, X.; Eisenberg, A. *Macromolecules* **1993**, *26*, 7339.
(35) Kjellander, R.; Florin, E. *J. Chem. Soc., Faraday Trans. 1* **1981**, *77*, 2053–2077.
(36) Preuschen, J.; Menchen, S.; Winnik, M. A.; Heuer, A.; Spiess, H. W. *Macromolecules* **1999**, *32*, 2690–2695.
(37) Siu, H.; Prazeres, J. V. T.; Duhamel, J.; Olesen, K.; Shay, G. *Macromolecules* **2005**, *38*, 2865–2875.
(38) Xia, Y.; Burke, N. A. D.; Stover, H. D. H. *Macromolecules* **2006**, *39*, 2275–2283.
(39) Weaver, J. V. M.; Bannister, I.; Robinson, K. L.; Bories-Azeau, X.; Armes, S. P.; Smallridge, M.; McKenna, P. *Macromolecules* **2004**, *37*, 2395–2403.
(40) Ringsdorf, H.; Venzmer, J.; Winnik, F. M. *Macromolecules* **1991**, *24*, 1678–1686.
(41) Chung, J. E.; Yokoyama, M.; Suzuki, K.; Aoyagi, T.; Sakurai, Y.; Okano, T. *Colloids Surf., B* **1997**, *9*, 37–48.
(42) Chung, J. E.; Yokoyama, M.; Aoyagi, T.; Sakurai, Y.; Okano, T. *J. Controlled Release* **1998**, *53*, 119–130.
(43) Kujawa, P.; Winnik, F. M. *Macromolecules* **2001**, *34*, 4130–4135.
(44) Kujawa, P.; Segui, F.; Shaban, S.; Diab, C.; Okada, Y.; Tanaka, F.; Winnik, F. M. *Macromolecules* **2006**, *39*, 341–348.
(45) Lodge, T. P.; Bang, J.; Hanley, K. J.; Krocak, J.; Dahlquist, J.; Sujan, B.; Ott, J. *Langmuir* **2003**, *19*, 2103–2109.
(46) Alexandridis, P.; Holzwarth, J. F. *Langmuir* **1997**, *13*, 6074–6082.
(47) Florin, E.; Kjellander, R.; Eriksson, J. K. *J. Chem. Soc., Faraday Trans. 1* **1984**, *80*, 2889–2910.
(48) Einarson, M. B.; Berg, J. C. *Langmuir* **1992**, *8*, 2611–2615.
(49) Ehrlich, S.; Wolff, N.; Schneiderman, R.; Maroudas, A.; Parker, K. H.; Winlove, C. P. *Biorheology* **1998**, *35*, 383–397.
(50) He, E.; Yue, C. Y.; Tam, K. C. *Langmuir* **2009**, *25*, 4892–4899.
(51) Huang, X.; Du, F.; Cheng, J.; Dong, Y.; Liang, D.; Ji, S.; Lin, S.-S.; Li, Z. *Macromolecules* **2009**, *42*, 783–790.